

**NUCLEAR DATA AND MEASUREMENTS SERIES**

**ANL/NDM-42**

**Fast Neutron Radiative Capture Cross Section of  $^{232}\text{Th}$**

by

W.P. Poenitz and D.L. Smith

March 1978

**ARGONNE NATIONAL LABORATORY,  
ARGONNE, ILLINOIS 60439, U.S.A.**

# NUCLEAR DATA AND MEASUREMENTS SERIES

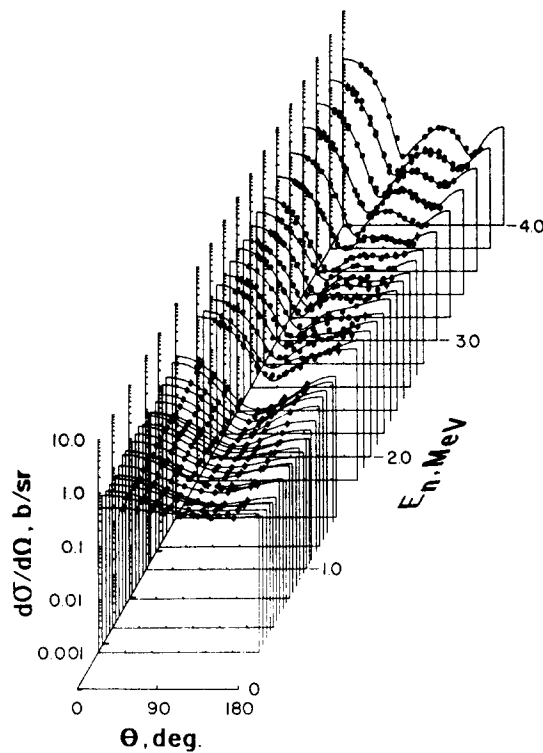
ANL/NDM-42

FAST NEUTRON RADIATIVE CAPTURE  
CROSS SECTION OF  $^{232}\text{Th}$

by

W. P. Poenitz and D. L. Smith

March 1978



U of C. AEA. USERDA

ARGONNE NATIONAL LABORATORY,  
ARGONNE, ILLINOIS 60439, U.S.A.

The facilities of Argonne National Laboratory are owned by the United States Government. Under the terms of a contract (W-31-109-Eng-38) between the U. S. Atomic Energy Commission, Argonne Universities Association and The University of Chicago, the University employs the staff and operates the Laboratory in accordance with policies and programs formulated, approved and reviewed by the Association.

#### MEMBERS OF ARGONNE UNIVERSITIES ASSOCIATION

The University of Arizona	Kansas State University	The Ohio State University
Carnegie-Mellon University	The University of Kansas	Ohio University
Case Western Reserve University	Loyola University	The Pennsylvania State University
The University of Chicago	Marquette University	Purdue University
University of Cincinnati	Michigan State University	Saint Louis University
Illinois Institute of Technology	The University of Michigan	Southern Illinois University
University of Illinois	University of Minnesota	The University of Texas at Austin
Indiana University	University of Missouri	Washington University
Iowa State University	Northwestern University	Wayne State University
The University of Iowa	University of Notre Dame	The University of Wisconsin

#### NOTICE

This report was prepared as an account of work sponsored by the United States Government. Neither the United States nor the United States Atomic Energy Commission, nor any of their employees, nor any of their contractors, subcontractors, or their employees, makes any warranty, express or implied, or assumes any legal liability or responsibility for the accuracy, completeness or usefulness of any information, apparatus, product or process disclosed, or represents that its use would not infringe privately-owned rights.

ANL/NDM-42

FAST NEUTRON RADIATIVE CAPTURE  
CROSS SECTION OF  $^{232}\text{Th}$

by

W. P. Poenitz and D. L. Smith

March 1978

In October 1977, the U. S. Energy Research and Development Administration (ERDA) was incorporated into the U. S. Department of Energy. The research and development functions of the former U. S. Atomic Energy Commission had previously been incorporated into ERDA in January 1975.

Applied Physics Division  
Argonne National Laboratory  
9700 South Cass Avenue  
Argonne, Illinois 60439  
USA

## NUCLEAR DATA AND MEASUREMENTS SERIES

The Nuclear Data and Measurements Series presents results of studies in the field of microscopic nuclear data. The primary objective is the dissemination of information in the comprehensive form required for nuclear technology applications. This Series is devoted to: a) measured microscopic nuclear parameters, b) experimental techniques and facilities employed in measurements, c) the analysis, correlation and interpretation of nuclear data, and d) the evaluation of nuclear data. Contributions to this Series are reviewed to assure technical competence and, unless otherwise stated, the contents can be formally referenced. This Series does not supplant formal journal publication but it does provide the more extensive information required for technological applications (e.g., tabulated numerical data) in a timely manner.

## TABLE OF CONTENTS

	<u>Page</u>
ABSTRACT. . . . .	1
I. INTRODUCTION. . . . .	2
II. PROMPT RADIATIVE CAPTURE CROSS SECTION MEASUREMENT. . . . .	4
A. Experimental Setup. . . . .	4
B. Measurements and Corrections. . . . .	5
III. ACTIVATION CROSS SECTION MEASUREMENT RELATIVE TO $^{235}\text{U}(n,f)$ . . . . .	7
A. Experimental Procedure. . . . .	7
B. Activity Detection and Calibration. . . . .	8
C. Gamma-Ray Absorption in Th Samples. . . . .	9
D. Corrections, Results and Uncertainties. . . . .	12
IV. ACTIVATION MEASUREMENT AT 30 keV. . . . .	14
V. DISCUSSION. . . . .	16
APPENDICES:	
I. THE THERMAL CROSS SECTION OF $^{232}\text{Th}(n,\gamma)$ . . . . .	17
II. GAMMA-BRANCHING RATIO OF THE 311-keV GAMMA RAY FROM $^{233}\text{Pa}$ DECAY . . . . .	18
ACKNOWLEDGEMENTS. . . . .	19
REFERENCES. . . . .	20
TABLES. . . . .	22
FIGURES . . . . .	24

FAST NEUTRON RADIATIVE CAPTURE CROSS  
SECTION OF  $^{232}\text{Th}^*$

by

W. P. Poenitz and D. L. Smith

Argonne National Laboratory  
Argonne, Illinois, U.S.A.

ABSTRACT

The  $^{232}\text{Th}(n,\gamma)$  cross section was measured between 30 keV and 2.5 MeV. A large liquid scintillator was used to measure the shape of the cross section relative to  $\text{Au}(n,\gamma)$  between 58 keV and 850 keV. The activation technique was used in measurements at 30 keV relative to  $\text{Au}(n,\gamma)$  and above 240 keV relative to  $^{235}\text{U}(n,f)$ . The activation results were utilized to normalize the shape data. The results agree well with recent experimental data by Lindner et al. and are substantially lower than the evaluated data file ENDF/B-IV in the several-hundred-keV range.

*\*This work supported by the U. S. Department of Energy.*

## I. INTRODUCTION

The radiative capture cross section of  $^{232}\text{Th}$  is of present interest due to its consideration as a fertile material in a  $^{232}\text{Th}/^{233}\text{U}$  breeding cycle. Most available data on  $^{232}\text{Th}$  are from rather old measurements and some corresponding values differ by more than a factor of 2 (see Ref. 1). Surprisingly, the two more recent measurements by Lindner et al. (2)-relative to  $^{235}\text{U}(n,f)$ - and by Macklin and Halperin (3)-relative to  $^6\text{Li}(n,\alpha)$ -differ by 10-20%. However, both cross section sets are substantially lower than the ENDF/B-IV evaluation (4) which is based upon the older data. The difference between the ENDF/B-IV evaluation and these recent measured values is 20-50% at 400 keV. Additional experimental evidence appears to be needed in view of these discrepancies and the importance of this cross section for technological applications.

Prompt gamma-ray detection with a large liquid scintillation detector has been successfully employed in  $(n,\gamma)$  measurements for many nuclides at this laboratory, but is hampered in the case of thorium by the high radioactivity of the sample and the low neutron binding energy which determines the total gamma cascade energy. At higher neutron energies an additional complication is encountered as a result of the emission of gamma cascades resulting from the fission process. However, shape data can be easily obtained by this method and the results then normalized with absolute values obtained by other techniques.

The activation technique is applicable in the determination of the  $^{232}\text{Th}(n,\gamma)$  cross section.  $^{233}\text{Th}$ , which results from the neutron capture of  $^{232}\text{Th}$ , decays with a half life of 22 min. to  $^{233}\text{Pa}$  which has a half life of 27 days (5) and is more convenient to measure than  $^{233}\text{Th}$ .

The present experiment included measurement of the energy dependence of the  $^{232}\text{Th}(n,\gamma)$  cross section relative to the  $^{197}\text{Au}(n,\gamma)$  standard cross section



using prompt gamma-ray detection techniques, measurement of the  $^{233}\text{Th}$  activation cross section relative to the  $^{235}\text{U}(n,f)$  standard cross section and a measurement, using also the activation technique, at 30 keV relative to the activation cross section of gold.

## II. PROMPT RADIATIVE CAPTURE CROSS SECTION MEASUREMENT

The shape of the  $^{232}\text{Th}(n,\gamma)$  cross section was determined relative to the  $\text{Au}(n,\gamma)$  cross section using a large liquid scintillator tank for the detection of the prompt gamma ray emission.

### A. Experimental Setup

The experimental setup, the neutron source, and the large liquid scintillator tank used to detect the prompt gamma rays have been described previously in detail (6-9); thus only a short summary of information relevant to the present experiment follows.

The  $^7\text{Li}(p,n)^7\text{Be}$  reaction was used at all energies. Measurements between 50 and 300 keV were carried out with a "pseudo-white" neutron spectrum produced by using a thick lithium target. Between 500 keV and 2 MeV measurements were carried out with "monoenergetic" neutrons using lithium targets which produced energy spreads of about 50-100 keV. The energy scale was based upon Hall-effect measurements of the magnet field of an analyzer magnet, calibrated using the threshold of the  $^7\text{Li}(p,n)$  reaction. The experimental setup was as shown in Fig. 1 of Ref. 3. The threshold for detection of capture gamma-ray events was 2.9 MeV. This rather high threshold (in reference to the binding energy of 4.79 MeV) reduced the background to a manageable level and excluded the detection of all  $(n,n'\gamma)$ - and  $(n,\gamma n')$ -events. A Grey Neutron Detector (10) was used as a relative flux monitor.

The thorium samples consisted of 0.03 cm thick strips of thorium metal of about 2.65 cm width and about 5.3 cm length. These strips were rather uneven, warped, and oxidized (another reason for not attempting an absolute normalization of these measurements). Similar-sized samples were made up of gold or carbon, the latter was used for background measurements.

## B. Measurements and Corrections

The shape of the ratio  $\sigma_{n,\gamma}(^{232}\text{Th})/\sigma_{n,\gamma}(^{197}\text{Au})$  was obtained between 50 keV and 300 keV by alternately irradiating the thorium and gold samples for 1 hour periods in a "pseudo-white" neutron spectrum. Twenty-five irradiations per sample were carried out. Equally many irradiations were carried out with the carbon sample. The monitor-count-rate ratios for the sum of the three sets of data were close to one. It was shown previously that variations of the neutron flux with energy did not occur in these measurements (7). No structure or other effects were found in the measurements with the carbon sample. This showed that capture of neutrons scattered into structural material of the capture detector was small. Background was subtracted after normalization of the time-of-flight spectra in a range outside the capture events. Ratios were formed over rather large intervals in order to improve the statistics of the data. "Monoenergetic" neutrons were used at energies  $\geq 500$  keV. Runs of 1-2 hours were sufficient at these energies. A time-of-flight condition was applied for background suppression.

Corrections were applied for transmission through the sample, elastic and inelastic scattering of neutrons within the samples and for the change of the efficiency of the detector with changing maximum energy of the  $\gamma$ -cascades. There is little energy dependence (<3%) for the ratio of the corrections for the capture of scattered neutrons (calculated by Monte Carlo techniques) in the thorium and the gold samples, thus the estimated uncertainty in the shape of the cross section due to this correction is small ( $\sim 1\%$ ). The  $\gamma$ -efficiency of the detector is rather uncertain; however, the energy dependence of the efficiency ratios varied only by  $\sim 3\%$  in the range covered by the white-spectrum measurements and by  $\sim 3.5\%$  in the range covered by the measurements with monoenergetic neutrons.

At higher energies, corrections were applied for the second neutron group obtained with the  ${}^7\text{Li}(p,n)$  reaction and for fission events in the thorium samples. The latter correction was obtained by normalizing the measured reaction rates at 2.5 and 3.0 MeV and extrapolating to the range  $<1$  MeV by utilizing the shape of the fission cross section (11).

The measured ratio was converted to a  $\text{Th}(n,\gamma)$  cross section shape by using ENDF/B-IV cross sections for  $\text{Au}(n,\gamma)$  (4). The two sets were independently normalized; the results are given in Table 3.

The major uncertainties for the shape data are due to the normalization (3.8% at 500 keV and 5.5% below from Section III) and the  $\text{Au}(n,\gamma)$  reference cross section (5.0%). Statistics is  $\sim 3\%$  and the systematical uncertainties  $\sim 2\%$ .

### III. ACTIVATION CROSS SECTION MEASUREMENT RELATIVE TO $^{235}\text{U}(n,f)$

The fast neutron fission cross section of  $^{235}\text{U}$  is a rather well-known reference cross section (12) and was used for all activation cross section measurements in this work except at 30 keV. The 30-keV measurement is discussed in Section IV.

#### A. Experimental Procedure

With the exception of one experimental point, all data were obtained with the thorium samples in a back-to-back geometry with the  $^{235}\text{U}$  deposits. The thorium samples were 0.013- or 0.020-cm-thick discs of metallic thorium (99.9%  $^{232}\text{Th}$ ) with a diameter of 1.588 cm. They were attached to the back of an ionization chamber (13) which had the  $^{235}\text{U}$  sample mounted on the same wall of the chamber. The spacing between these samples was determined by the thickness of the ionization chamber wall (0.013 cm of iron) and of the backing of the  $^{235}\text{U}$  sample (0.013 cm of stainless steel). In one measurement, the thorium sample was sandwiched between two uranium deposits of approximately equal mass inside the ionization chamber. Though this arrangement leads to more tedious experimental procedures, it has the advantage of reducing geometrical corrections and corrections for scattering of neutrons within the samples, the sample backings and the ionization chamber (14). Several  $^{235}\text{U}$ -deposits were used as summarized in Table 1. Measurements at  $\sim 500$  keV were carried out with the samples at a distance of 2.5, 5, and 10 cm from the neutron source. All other measurements were performed at a distance of 2.5 cm. All irradiations were performed with the samples perpendicular to the proton beam axis at zero degrees. Irradiation times were in the range of 3 to 12 hours. Neutron energy spreads were between 50 and 200 keV for most irradiations.

The thorium sample activities were measured with a coaxial Ge(Li) detector after allowing sufficient time for the 22 min.  $^{233}\text{Th}$  activity to

decay to  $^{233}\text{Pa}$ . The samples were counted at a distance of  $\sim 0.9$  cm from the front of the Ge-diode. The yield of the 311-keV gamma ray from the decay of  $^{233}\text{Pa}$  was utilized to calculate the total  $^{232}\text{Th}$  activation.

#### B. Activity Detection and Calibration

The factor relating the counted 311 keV  $\gamma$ -rays to the number of  $^{233}\text{Pa}$  decays was obtained by three different techniques:

a) The decay rate of a  $^{237}\text{Np}$  sample was measured by low-geometry  $\alpha$ -counting. The  $\alpha$ -decay of  $^{237}\text{Np}$  leads to  $^{233}\text{Pa}$ ; thus, if in equilibrium, the measurement of this sample yields the calibration factor. However, a correction for  $\gamma$ -ray attenuation in the thorium sample must be applied.

b) The thermal-neutron activation cross section of thorium is very well known ( $7.40 \pm .08$  b, Ref. 15). A sandwich consisting of a thin gold foil between two thorium foils was activated in a thermal neutron field (Cd-ratio 4000). The neutron flux was determined from the activity induced in the gold sample (thermal cross section  $98.8 \pm 0.3$  (15)). The activity of the latter was measured by  $4\pi\beta$ - $\gamma$  coincidence counting; corrections were applied as described elsewhere (16). Correction for the non- $1/v$  energy dependence of the gold and the thorium cross sections were applied using the Westcott factors (17). Corrections for shielding effects in the sandwich were applied. The activity of the thorium samples was measured with the Ge(Li) detector and this provided a calibration factor which already included the effective  $\gamma$ -ray absorption.

c) The  $\gamma$ -ray detection efficiency of the Ge(Li) detector at 311 keV was determined by an absolute calibration at 411 keV using a  $4\pi\beta$ - $\gamma$ -coincidence-calibrated Au sample and a relative shape curve deduced from measurements on a variety of other  $\gamma$ -ray sources. The calibration factor was then calculated assuming a value of 0.377 for the probability of 311-keV  $\gamma$ -ray emission per

decay of  $^{233}\text{Pa}$  (5). The value obtained with this technique requires a correction for the effective  $\gamma$ -ray absorption in the thorium samples and consideration of  $\gamma$ -ray sum coincidence effects.

The values obtained from the three techniques were (for an infinitesimally thin Th sample)

(a)  $0.01430 \pm 0.00020$ ,

(b)  $0.01412 \pm 0.00024$ ,

(c)  $0.01353 \pm 0.00081$ ,

for which the weighted average is:

$$0.01420 \pm 0.00012.$$

The activities of all the samples were measured 2-4 times each over a period of one to two half lives.

### C. Gamma-Ray Absorption in Th Samples

There are a number of effects which influence the detection probability for the 311-keV  $\gamma$ -ray. These effects were treated together as an "effective  $\gamma$ -ray absorption" and were determined experimentally. However, an effort was made to understand each of the effects involved. The effective  $\gamma$ -ray absorption was measured for both of the sample thicknesses used in the present experiment. The measurements were carried out using a  $^{237}\text{Np}$  sample. The intensity of the 311-keV  $\gamma$ -ray emitted from the sample was measured in two positions which differed only by the Th-sample thickness. The average of these measurements provided the effective activity at the center-of-the-Th-sample position exclusive of  $\gamma$ -ray absorption or other effects. These measurements were then repeated with a non-activated Th sample placed in front of the  $^{237}\text{Np}$  sample (when the latter was farther away from the Ge(Li) detector) and behind the  $^{237}\text{Np}$  sample (when the latter was closer to the Ge(Li) detector). The

average of the two measurements provided the effective activity of the Th sample at the center of the Th sample with  $\gamma$ -ray attenuation and appropriate other effects included.

It was assumed that the measurement for the midplane of the thorium sample represents the effective  $\gamma$ -ray attenuation for a homogeneously activated sample. This approximation is expected to be adequate as the total effect is less than 10% (thus, for example, the exponential attenuation might be replaced by a linear term with no more than 0.5% error). The experimentally determined effective  $\gamma$ -ray attenuation was found to agree well with that calculated by considering the attenuation of a parallel  $\gamma$ -ray flux in a foil of half the actual thickness. This is a coincidence as it would be expected that the actual  $\gamma$ -ray losses due to absorption or incoherent scattering would be much larger because of the larger average sample thickness applicable to the detection position of the sample as a result of the large counting solid angle. A Monte Carlo calculation for the first collision probability of  $\gamma$ -rays in the Ge(Li) detector (18) yielded a 3.5%-larger value for the  $\gamma$ -ray attenuation than the experimental value for a  $.25 \text{ g/cm}^2$  sample. Effects which might explain the difference are:

(a) Coherent in-scattering reduces the  $\gamma$ -ray attenuation. This reduction should be expected to be larger than suggested by the ratio of coherent to total cross section because the in-scattering comes from parts of the sample with larger effective thickness than applicable to the  $\gamma$ -ray attenuation. A Monte Carlo calculation of the effect suggests an  $\sim 1\%$  reduction for  $.25 \text{ g/cm}^2$ . However, results from attempted measurements of the in-scattering effect were inconclusive.

(b) Total  $\gamma$ -ray attenuation cross sections (19) are supposed to be uncertain by  $\sim 10\%$ . This might account for as much as  $\sim 1\%$  in the difference between the calculated and the measured absorption. We measured the  $\gamma$ -ray attenuation of



thorium for a parallel  $\gamma$ -ray flux using several  $\gamma$ -lines from the decay of  $^{133}\text{Ba}$ . The results agreed within  $\sim 2\%$  with the listed total  $\gamma$ -ray attenuation cross sections. This virtually eliminated the possibility of photon cross section uncertainty as an explanation for part of the observed difference.

(c) The observed 311-keV  $\gamma$ -ray depopulates a level at 311 keV by transitions to the groundstate. The transition probability is 71% per decay of  $^{233}\text{Pa}$ , about half of which is electron-converted. Beta decay of  $^{233}\text{Pa}$  populates this level with a probability of only 17%. The remaining 54% come from de-excitations through higher-excited states.

The feeding of the 311-keV level from higher-lying levels leads to sum-coincidences with the 311-keV transition which reduce the counting probability of this  $\gamma$ -ray. However, all transitions feeding the 311-keV level have substantially lower energy and are thus much more likely to be absorbed in the thorium sample. This reduces the probability for coincidences and thus enhances the counting probability for the 311-keV  $\gamma$ -ray. An estimate of the net effect suggests that the counting probability of the 311-keV  $\gamma$ -ray should only be reduced by about 1%. Thus, this effect would not explain the observed difference between calculated and measured  $\gamma$ -ray attenuation. However, this estimate is based upon uncertain electron conversions for the transitions from the higher-lying levels.

The sum-coincidences should lead to pulses which fall in a range  $\sim 103$  keV above the observed 311-keV photopeak. Thus we measured the ratio of the counts of an interval around the 311-keV peak and counts from an interval covering  $\sim 120$  keV above this peak. This ratio was measured at the normal counting position and at a distance of 10 cm where geometrical factors should reduce sum-coincidences to a negligible amount. The result of this measurement was that the counting probability for the 311 keV might be reduced by as much as 10% owing to sum-coincidences. Such a large amount could explain most of the

difference between the observed effective  $\gamma$ -ray attenuation and the calculated one. However, the reproducibility of this measurement was not very good and the interpretation of the result is not unique (for example, the photopeak-to-Compton ratio may change with distance from the detector and this would produce an artificial effect).

#### D. Corrections, Results and Uncertainties

The detected fission counts were corrected for bias (1-2%) and total fission fragment absorption (0.6-2.5%, Ref. 20). Effects due to neutrons scattered in the neutron-source structural material, the fission counter and the sample backings were calculated with a Monte Carlo code (21) and found to be in the range of 0.2-3.8%. The cross sections and average energies were calculated taking into account the angular distribution of the source reaction, the different sample sizes, distance from the source, path through the sample, neutron flux as a function of energy and transmission through the thorium sample backings (parameters and techniques from Ref. 22). An independent calculation of these effects was made using different parameters for the source reaction (Ref. 23) and somewhat different techniques. The two results agreed within  $\sim 1\%$ .

The cross sections obtained at 500 keV neutron energy for the various experimental configurations investigated are given in Table 2. The average neutron energy values were somewhat different for these various measurements and corrections were applied in order to permit a comparison of these results at a reference energy of 500 keV. Table 2 shows that all these corrected values agree to within one standard deviation with the average value of  $\sigma(500 \text{ keV}) = .1549 \pm 0.0059$  which is included in Table 3. This value was used for the normalization of the monoenergetic prompt capture  $\gamma$ -ray detection data. Values at all other energies are also given in Table 3. The 244-keV value was

used to normalize the low-energy white source time-of-flight shape measurements. Values obtained with the activation technique are labeled with an "A" and those obtained with prompt  $\gamma$ -ray detection technique are labeled with "T" in Table 3. The statistical uncertainties are also given in Table 3. The systematic uncertainties common to all the activation measurements are: 1.0% for the mass of the fissile deposit, 0.9% for the Ge(Li)-detector counting efficiency, 0.5% for the thorium sample mass, 0.5% for the half-life of  $^{233}\text{Pa}$ , and 3.0% for  $\sigma_f$  of  $^{235}\text{U}$ . The ranges for other uncertainties are 0.6-1.0% for  $\gamma$ -ray absorption in the thorium samples, 0.1-0.8% for the neutron multiple scattering corrections, 0.5-2.0% for background subtraction, and 0.5-1.6% for effects related to the sample geometry and neutron-source anisotropy. Uncertainty estimates for other corrections and effects are usually small: Dead-time correction for fission counting, 0.2%, statistics of fission counting, 0.2%, and  $\gamma$ -ray counting distance reproducibility, 0.5%.

## IV. ACTIVATION MEASUREMENT AT 30 keV

A kinematically-collimated neutron beam with an average energy of  $\sim 30$  keV may be obtained with the  ${}^7\text{Li}(p,n){}^7\text{Be}$  source reaction using a primary energy at  $\sim 2$  keV above the reaction threshold. The energy and sample angle were such that the beam cone diameter was less than the sample diameters. In order to avoid problems and uncertainties associated with a possible inhomogeneous distribution of fissile material, the measurement at 30 keV was carried out relative to the  $\text{Au}(n,\gamma)$  cross section instead of the  ${}^{235}\text{U}(n,f)$  cross section. The  $\text{Au}(n,\gamma)$  cross section at 30 keV ( $0.576 \pm 0.017$  b) is rather well known (24, 25), and the Au-capture rate can be determined by the activation technique with less than 1% uncertainty. Homogeneous metal samples can easily be obtained. A 0.020-cm-thick metallic Th sample and a 0.025-cm-thick metallic Au sample of the same diameter were irradiated back-to-back and perpendicular to the neutron beam for  $\sim 8$  h. The detection of the  ${}^{233}\text{Pa}$  activity of the thorium sample was as discussed in Section III. The  ${}^{198}\text{Au}$  activity was measured with the same Ge(Li) detector which was calibrated with a calibrated Au foil. The activity of this calibration sample was measured absolutely with the  $4\pi\beta\text{-}\gamma$ -coincidence technique.

The  $\gamma$ -ray absorption of the gold disc was measured in an experiment similar to the one described for the thorium samples in Section III; other corrections were small for this experiment. Background was negligible due to the fact that the kinematically-collimated neutrons go through the samples and do not hit the largest scatterer, the floor, as they do at other energies. Corrections for path lengths in the sample, neutron angular distribution, geometry effects etc. do not apply because all neutrons go through both samples in identical fashion. The net correction for scattered neutrons and self shielding is small for the measured ratio (0.3%), though the corrections for the individual samples are in the 2-3% range.

The result from this measurement is also given in Table 3. The major uncertainties are due to the counting statistics of the  $^{233}\text{Pa}$  activity, and the Au-cross section (3%). Other uncertainties are similar to those stated above for the activation measurements relative to  $^{235}\text{U}(n,f)$ , and are usually small (<1%).

## V. DISCUSSION

The results of the present measurements, which are summarized in Table 3, are shown in Fig. 2 and also are compared with two evaluations. The present experimental data agree best with a recent evaluation which utilized all available ratios to  $^{238}\text{U}(n,\gamma)$ ,  $\text{Au}(n,\gamma)$ ,  $^{235}\text{U}(n,\gamma)$  and  $^6\text{Li}(n,\alpha)$  (11). These experimental data do appear to be higher by more than one standard deviation, above 1 MeV. The present data are compared in Fig. 2 with the two most recent experimental data sets--by Lindner et al. (2) and Macklin and Halperin (3). The present data agree well within uncertainty limits with the data by Lindner et al.; however, they seem to be systematically higher.

## Appendix I

THE THERMAL CROSS SECTION OF  $^{232}\text{Th}(n,\gamma)$ 

The three independent techniques for calibration of the Ge(Li) detector may be utilized to derive the thermal cross section of  $^{232}\text{Th}(n,\gamma)$ . The weighted average of the two normalization techniques which do not involve the thermal cross section (a,c) is

$$0.01426 \pm .0017.$$

Comparing this with the measurement based on the thermal activation yields a thermal cross section for  $^{232}\text{Th}(n,\gamma)$  of

$$7.33 \pm 0.17 \text{ b.}$$

This value is in good agreement with the averaged value of  $7.40 \pm 0.08 \text{ b}$  stated in Ref. 15.

## Appendix II

GAMMA-BRANCHING RATIO OF THE 311 keV  $\gamma$ -RAY FROM  $^{233}\text{Pa}$  DECAY

Another quantity which may be derived from the three independent calibration values for the Ge(Li) detector is the 311 keV  $\gamma$ -emission probability for the  $^{233}\text{Pa}$  decay. The value obtained from the data in Section III is

39.5  $\gamma$ 's per 100 decay ( $\pm 6\%$ ).

An additional measurement was made with the Np-sample at a larger distance from the detector (25 cm) (thus reducing the number of sum coincidences) and a Cs-source for its absolute calibration. The value obtained from this measurement was

37.73  $\gamma$ 's per 100 decay ( $\pm 6\%$ ).

The weighted average from these two values is

38.6  $\gamma$ 's per 100 decay ( $\pm 3.8\%$ ).



## ACKNOWLEDGEMENTS

Metallic thorium samples for the prompt  $\gamma$ -ray detection measurements were provided by R. L. Macklin (Oak Ridge National Laboratory). R. Armani provided the  $^{237}\text{Np}$ -samples and carried out the thermal flux irradiations. Valuable discussions with J. W. Meadows and G. J. DiIorio are gratefully acknowledged.

## REFERENCES

1. D. I. Garber and R. R. Kinsey, "Neutron Cross Sections, Vol. II, Curves," BNL-325, Third Edition, Brookhaven National Laboratory (1976).
2. M. Lindner, R. J. Nagle and J. H. Landrum, Nucl. Sci. Eng. 59, 381 (1976).
3. R. L. Macklin and J. Halperin, Nucl. Sci. Eng. 64, 849 (1977).
4. "Evaluated Nuclear Data File ENDF/B-IV," see ENDF-102, Brookhaven National Laboratory (1975).
5. "Nuclear Data Sheets for A = 233," Yurdanur A. Ellis, Oak Ridge National Laboratory (1971).
6. W. P. Poenitz, "Fast Neutron Capture and Activation Cross Sections of Niobium Isotopes," ANL/NDM-8, Argonne National Laboratory (1974).
7. W. P. Poenitz, Nucl. Sci. Eng. 57, 300 (1975).
8. W. P. Poenitz, "Radiative Capture of Fast Neutrons in  $^{165}\text{Ho}$  and  $^{181}\text{Ta}$ ," ANL/NDM-15, Argonne National Laboratory (1975).
9. W. P. Poenitz, Proc. Conf. Nuclear Cross Sections and Technology, NBS SP 425, 901 (1975).
10. W. P. Poenitz, Nucl. Instr. Methods 58, 39 (1968), and 72, 120 (1969).
11. J. Meadows, W. Poenitz, A. Smith, D. Smith, J. Whalen and R. Howerton, "Evaluated Nuclear Data File of Th-232," ANL/NDM-35, Argonne National Laboratory (1978).
12. NEANDC/NEACRP Specialists Meeting on Fast Neutron Fission Cross Sections of U-233, U-235, U-238 and Pu-239, ed. W. P. Poenitz and A. B. Smith, ANL-76-90, Argonne National Laboratory (1976).
13. J. W. Meadows, Nucl. Sci. Eng. 49, 310 (1972).
14. W. P. Poenitz, Nucl. Sci. Eng. 40, 383 (1970).
15. "Neutron Cross Sections, Vol. I, Resonance Parameters," S. F. Mughabghab and D. I. Garber, BNL-325, Third Edition, Vol. I, Brookhaven National Laboratory (1973).
16. W. P. Poenitz, "Determination of Absolute Thermal Neutron Flux by Gold Foils," KFK-180, Nuclear Research Center Karlsruhe (1963).
17. C. H. Westcott, "Effective Cross Section Values for Well-Moderated Thermal Reactor Spectra," CRRP-787, Chalk River Laboratory (1958).
18. J. W. Meadows, Argonne National Laboratory, private communication (1978).
19. E. Storm and H. I. Israel, Nucl. Data Tables A7, 565 (1970).

20. J. W. Meadows, "The Fission Cross Section of  $^{239}\text{Pu}$  Relative to  $^{235}\text{U}$  from 0.1 to 10 MeV, ANL/NDM-39, Argonne National Laboratory (1978).
21. D. L. Smith and J. W. Meadows, "Neutron Inelastic Scattering Studies for Lead-204," ANL/NDM-37, Argonne National Laboratory (1977).
22. D. L. Smith and J. W. Meadows, "Neutrons from Proton Bombardment of Natural Lithium," ANL-7938, Argonne National Laboratory (1972).  
Also, Donald L. Smith and James W. Meadows, "Measurement of  $^{58}\text{Ni}(n,p)^{58}\text{Co}$  Reaction Cross Sections for  $E_n = 0.44-5.87$  MeV Using Activation Methods," ANL-7984, Argonne National Laboratory (1973).
23. H. Liskin and A. Paulsen, "An Evaluation for Cross Sections of the Reaction  $^7\text{Li}(p,n)^7\text{Be}$  and  $^7\text{Be}^*$ ," EANDC (E)-159 "L," Central Bureau for Nuclear Measurements, Geel, Belgium (1973).
24. W. P. Poenitz, "Interpretation and Intercomparison of Standard Cross Sections," Proc. Symp. on Neutron Standards and Flux Normalization, AEC Symposium Series 23, Argonne National Laboratory (1971).
25. R. L. Macklin, J. Halperin, and R. R. Winters, Phys. Rev. C11, 1270 (1975).

TABLE 1. Summary of  $^{235}\text{U}$ -Samples Used in the Present Experiment

Label	Isotopic Composition, %				Atoms U
	$^{234}\text{U}$	$^{235}\text{U}$	$^{236}\text{U}$	$^{238}\text{U}$	
U5-5-1	1.034	98.409	0.455	0.102	$2.690 \cdot 10^{18}$
U5-5-2	1.034	98.409	0.455	0.102	$2.102 \cdot 10^{18}$
ST1	0.8556	93.244	0.3321	5.560	$1.676 \cdot 10^{18}$
ST5	0.8556	93.244	0.3321	5.560	$1.056 \cdot 10^{18}$

TABLE 2. Experimental Results at  
 $\sim 500$  keV Neutron Energy

Parameter	$\sigma(500 \text{ keV}), \text{ b}$	$\frac{\Delta\sigma}{\sigma}, \%$
Distance 2.54 cm	0.1536	2.4
Distance 5.08 cm	0.1508	2.7
Distance 10.16 cm	0.1518	4.7
Th-Sample Thickness	0.1570	2.5
Sandwich Experiment	0.1577	3.3

TABLE 3. Summary of Experimental Results for  
the  $^{232}\text{Th}(n,\gamma)$  Cross Section

$E_n$ , MeV	Uncertainty in $E_n$ , MeV	Resolution, MeV	$\sigma$ , b	$\pm\Delta\sigma$ , b	Statistical Uncertainty, %	Technique, Reference Cross Section
0.030	0.001	0.013	0.464	0.028	4.7	A, Au <sup>a</sup>
0.244	0.006	0.038	0.147	0.006	1.2	A, U-235
0.500	0.010	0.055	0.155	0.006	0.4	A, U-235
0.622	0.011	0.052	0.180	0.008	1.4	A, U-235
1.013	0.011	0.057	0.137	0.006	1.4	A, U-235
1.497	0.010	0.049	0.111	0.005	2.5	A, U-235
1.984	0.012	0.050	0.076	0.008	10.5	A, U-235
2.480	0.015	0.080	0.050	0.003	3.6	A, U-235
0.0584	0.005	0.0032	0.377	0.031	3.0	T, Au <sup>b</sup>
0.0648	↓	0.0035	0.340	0.028	↓	↓
0.0724	↓	0.0040	0.303	0.025	↓	↓
0.0810	↓	0.0049	0.251	0.021	↓	↓
0.105	↓	0.0072	0.216	0.018	↓	↓
0.121	↓	0.0090	0.211	0.017	↓	↓
0.141	↓	0.012	0.200	0.016	↓	↓
0.167	↓	0.015	0.192	0.016	↓	↓
0.200	↓	0.019	0.172	0.014	↓	↓
0.244	↓	0.026	0.142	0.012	↓	↓
0.305	↓	0.035	0.152	0.012	↓	↓
0.50	0.01	0.03	0.155	0.011	↓	↓
0.60	↓	0.03	0.168	0.012	↓	↓
0.70	↓	0.03	0.177	0.013	↓	↓
0.85	↓	0.03	0.166	0.012	↓	↓

<sup>a</sup>A = Activation measurements.

<sup>b</sup>T = Large liquid scintillator measurements.

